Dipole Antenna with 18 × 5 Square Electromagnetic Band Gap for Applications Used in Monitoring Children Trapped in Cars

Watcharaphon Naktong[1] and Natchayathorn Wattikornsirikul[2, *]

Abstract—This article presents the design of a dipole antenna structure in combination with a square electromagnetic band gap (EBG) to monitor the children trapped in cars using a 750 MHz frequency band which responds the most to human movement detection. The antenna structure was designed on a copper plate with a thickness of 0.297 mm and polyester mylar film baseplate with a thickness of 0.3 mm and dielectric value of 3.2. By design, the dipole antenna had a size of $201.56 \times 12.5 \, \text{mm}^2$ and 18×5 units square electromagnetic band gap (EBG) of size $254.64 \times 71.86 \, \text{mm}^2$. The results of the measurement showed that the bandwidth impedance in the operating frequency range was 4.78% (735–771 MHz) with a gain of 6.3 dBi. There was an omnidirectional signal transmission. The dipole antenna had the best distance between the EBG plates of 30 mm. When being examined at a distance of 500–1,600 mm, it was the most effective at an average signal strength of approximately 0.032 mW every time there was movement of a human body in the car.

1. INTRODUCTION

Nowadays, there is a lot of news about children being trapped in cars because parents rushed to run errands and forgot that there were children in the car causing the children's death due to suffocation and the heat inside the car [1–4]. Such problems affect families in Thailand and abroad. This problem has become continually chronic because no company has created a monitoring system in cars to fix the problem. Apart from burglar alarm system, most cars do not have a child or pet alarm system. Based on the aforementioned events, researchers were interested in using radio frequency devices to develop, design, and build a system to monitor human body movements in cars [5–7]. The device was used as a transmitter and electromagnetic band gap to reduce the reflection distance of a car's steel roof to help reduce the size of the detector. Based on the above, a researcher selected a dipole antenna structure with a U-shaped stub enhancement technique on both sides for 920 MHz RFID frequency range which was compatible with rectangular electromagnetic frequency band plates. With EBG placed at a distance of 1 mm from the antenna, the gain ranged from 6.1 to 8.2 dBi [8]. A dipole antenna with U-shaped stub enhancement technique on both sides for use in the 1.39–2.09 GHz frequency range was compatible with 2×2 units cross grooving circular electromagnetic frequency band plate. With EBG placed at a distance of 16.3 mm from the antenna, the gain ranged from 6.1 to 8.2 dBi [9]. A rectangular loop dipole antenna with the technique of adding U-shaped stubs on both sides for use in the frequency range 2.425–2.625 GHz was compatible with electromagnetic band plates mushroom-like 18×18 units. With EBG placed at a distance of 20.75 mm from the antenna, the gain was 1.23 dBi [10]. A dual-polarized crossed dipole antenna for the use in the 2.9–3.32 GHz frequency range, compatible with 6×6 units rectangular electromagnetic band plates was placed at a distance of 15 mm from the 1st and 2nd dipole

[1] Department of Telecommunications Engineering, Faculty of Engineering and Technology, Rajamangala University of Technology Isan, Nakhon Ratchasima 30000, Thailand. [2] Department of Electronics and Telecommunications Engineering, Faculty of Engineering, Rajamangala University of Technology Phra Nakhon, Bangkok 10300, Thailand.

antennas [11]. A dual-polarized antenna, using the technique of adding the stub main radiator on both sides for the use at port 1 with a frequency range of 32% (3.04–4.21 GHz) and port 2 with a frequency range of 28.3% (3.13–4.16 GHz), was compatible with concentric rectangular ring electromagnetic band gap (CRR-EBG) 8×8 units. With EBG placed at a distance of 28 mm from the antenna, the gain can be increased by 5 dBi [12]. A rectangular loop antenna for harvesting, operated at a voltage of 868 MHz, ISM standard was compatible with 3×3 units rectangular electromagnetic band plate. With EBG placed at a distance of 42.3 mm from the antenna and with a gain of 7.52 dBi, a voltage of 1.4 V could be harvested [13]. A dipole antenna for use at 4.3–7.6 GHz was compatible with 17×17 units quad bend triangular resonator (QBTR) electromagnetic band plates. With EBG placed at a distance of 1.524 mm from the antenna, it had a gain of 5 dBi which radiated energy in a directional radiation pattern [14]. A dipole antenna operating at 1.45 THz was combined with a star-shaped artificial magnetic conductor (AMC) plate of 18×18 units. With EBG placed at a distance of 3 mm from the antenna the gain value ranged 2.7–4.15 dBi which radiated energy in a directional radiation pattern [15]. A meandered dipole antenna for the use at 19–36 MHz was compatible with 18×18 units of artificial magnetic conductor (AMC) band plates. With EBG placed at a distance of 18 mm from the antenna, a gain value ranged from 22.20 to 16 dBi which radiated energy in a directional radiation pattern [16]. A shared-aperture Fabry-Perot cavity antenna (FPCA) for the use at 3.45 GHz and 5 GHz was combined with partially reflective surface (PRS), 8×8 units frequency selective surface (FSS) electromagnetic band plates. Arranged at a distance of 34.5 mm from the antenna, they had gains of 13.7 dBi and 16.8 dBi, respectively, which radiated energy in a directional radiation pattern [17]. An E-shaped dipole antenna with a two-layer rectangular grooving technique, for use in the frequency range 4.48–7.12 GHz, WLAN/WiMAX, and MIMO 2×2 systems was compatible with 3×3 units artificial magnetic conductor (AMC) band plates. With EBG placed at a distance of 3 mm from the antenna, a gain of 8.4 dBi was obtained, and it radiated energy in a directional radiation pattern [18]. A low-profile 16-element printed dipole antenna (PDA) 8×8 units MIMO system for use in the 4.50–7.20 GHz frequency range and WLAN/WiMAX was compatible with 12×12 units of artificial magnetic conductor (AMC) band plates. With EBG placed at a distance of 4 mm from the antenna, a gain of 8 dBi was obtained [19]. A Dual-Band Circularly Polarized Crossed-Dipole Antenna Backed for 2.31–2.56 GHz frequency range and 5.44–6 GHz WLAN system was compatible with 5×6 units artificial magnetic conductor (AMC) band plates. With EBG placed at a distance of 14 mm from the antenna, there were gains of 5.1 dBic and 7.41 dBic, respectively, which radiated energy in a directional radiation pattern [20]. A low-profile linearly polarized antenna based for operating at frequency range of 4.77–7.12 GHz UWB system was compatible with 6×6 units artificial magnetic conductor (AMC) band plates. With EBG placed at a distance of 4 mm from the antenna, there were gains of 9.9 dBi, respectively, and it radiated energy in a directional radiation pattern [21]. A four arrow-shaped dipole antenna for use in the frequency range 3.04–4.70 GHz was compatible with electromagnetic band plates mushroom-like type 10×10 units and had the gain of one antenna equal to 10.06 dBi and two antennas equal to 9.89 dBi [22]. A C-shaped monopole antenna structure for use in the frequency range 2.45 GHz in WiFi system was compatible with 2×2 units of a non-equilateral triangle electromagnetic frequency band plate. With EBG placed at a distance of 100 mm from the antenna, there was a gain of 6.55 dBi. Four wearable antennas for on-body applications monitored skin at 13 mm, obesity at 20 mm, muscle at 5 mm, and bone at 2 mm. When these were examined in the human body, the energy values were $1,008 \, \text{kg/m}^3$, $1,006 \, \text{kg/m}^3$, $900 \, \text{kg/m}^3$, and $1,001 \, \text{kg/m}^3$, respectively [23]. A rectangular monopole antenna for mounting on jeans for use in the frequency range 3.5–12.4 GHz in the UWB system was compatible with 7×7 units square electromagnetic frequency band plate. With EBG placed at a distance of 7.9 mm from the antenna, there was a gain of 9.1 dBi with directional radiation pattern [24]. A rectangular monopole antenna for mounting on jeans for use in the frequency range 6.5 GHz in the C-band system was compatible with 2×2 units square electromagnetic frequency band with double C-shaped grooving. With EBG placed at a distance of 0.8 mm from the antenna, there was a gain of 8.51 dBi with a directional pattern of energy radiation [25]. A circular monopole antenna for use in the frequency range 2.45 GHz in WiFi system was compatible with a 3×3 units square electromagnetic frequency band plate. With EBG placed at a distance of 1 mm from the antenna, there was a gain of 6.8 dBi and radiated energy in a directional radiation pattern [26]. A rectangular monopole antenna for use in the frequency range 2.45 GHz and 5.20 GHz in WiFi system was compatible with 3×3 units of non-equilateral triangle

electromagnetic frequency band plate. With EBG placed at a distance of 1.4 mm from the antenna, there was a gain of 13 dBi and radiated energy in a directional radiation pattern [27]. A circular monopole antenna for use in the frequency range 2.45 GHz, 2.65 GHz, and 5.20 GHz in the WiFi system worked with 3×3 units of composite right/left-handed transmission lines (CRLH TL) electromagnetic frequency band plate. With EBG placed at a distance of 1.5 mm from the antenna, there were gains of 4.25 dBi, 2.99 dBi, and 2.3 dBi, respectively, and radiated energy in a directional radiation pattern [28]. A coplanar flexible antenna for use in the frequency range 2.45 GHz in WiFi system was compatible with composite right/left-handed transmission lines (CRLH TL) electromagnetic frequency band plate type 4×3 units. With EBG placed at a distance of 1.5 mm from the antenna, there was a gain of 4.25 dBi, and, when being examined in the human arm, an energy value of 0.0344 W/kg [29]. A rectangular monopole antenna using a two-layer rectangular grooving technique for use in the frequency range 2.45 GHz, 3.50 GHz, and 5.80 GHz in the WiFi system was compatible with Textile EBG-Based electromagnetic frequency band plate type 2×2 units. Three wearable antennas for on-body applications monitored skin at 1 mm, obesity at 5 mm, and muscle at 40 mm. The gains were 5.11 dBi, 6.43 dBi, and 7.41 dBi, which, when being examined in the human body, were 0.47 W/kg, 0.86 W/kg, and 0.14 W/kg, respectively [30]. An open rectangular antenna using rectangular grooving technique with an added L-shaped stub for use in the 4.09–4.52 GHz frequency range was compatible with 2×3 units oval electromagnetic band plates. It was placed at a distance of 1.5 mm from 3 antennas for use in a left hand circular polarization (LHCP) radiation form [31]. A rectangular microstrip antenna using rectangular grooving technique for use in the frequency range 402–405 MHz was compatible with 2×2 units circular electromagnetic frequency band plate. Four wearable antennas for on-body applications monitored skin at 2 mm, obesity at 5 mm, muscle at 20 mm and bone at 13 mm. When being examined in the human body, the energy values were 1,620 W/m^3, 300 W/m^3, 480 W/m^3, and 610 W/m^3, respectively [32]. A triangular microstrip antenna using rectangular grooving technique for use in the 2.38 GHz frequency range was compatible with 2×2 units electromagnetic frequency band plates. Two wearable antennas for on-body applications monitored were placed at 1 mm and 2 mm, had the energy values of 0.306 W/kg, 0.640 W/kg, and 0.565 W/kg, respectively, with a gain of 7.80 dBi when being examined at the human body [33]. Based on the above research, the researchers were interested in developing a dipole antenna structure [14, 15] together with EBG square electromagnetic band plate. The distance between antennas was reduced [11, 22, 24], which had the advantage of being simple in both structures and by examining the movement of the human body in the car.

In the calculation, the antenna structure results were simulated and compared with the measurement results together with the simulation of the effect of the electric field (E-plane) and magnetic field (H-plane) reflection coefficients. The antenna gain is presented in Section 2, the electromagnetic wave test monitoring human body movements in cars in Section 3. Section 4 presents the comparison of antenna results with electromagnetic frequency band plates with past research. The final Section 5, summarizes the research.

2. ANTENNA STRUCTURE DESIGN AND ANTENNA PROPERTIES MEASUREMENT

2.1. Design of Antenna Structure

The antenna structure design used a basic dipole antenna structure [34, 35]. The antenna was used to detect human body movements in the operating frequency range 150–1,500 MHz and monitor the actual range of 500 mm, 1,100 mm, and 1,600 mm with a signal strength of 0.032 mW (-15 dBm). An actual car was used in the measurement to find the most responsive frequency. From the test, the most responsive frequency band to the movement of the was 750 MHz as shown in Figure 1. The structure of a dipole antenna was designed on a copper sheet where the thickness of the base material (t_{ant}) was 0.297 mm; the conductivity of the conductor material (σ) was 5.8×10^7 S/m; the polyester mylar film base plate thickness (h_1) was 0.3 mm; and dielectric (ε_r) was 3.2. By design, the dipole antenna was 201.56×12.5 mm^2 as shown in Figure 2. It can be calculated as in Equations (1)–(3). The figure of the dipole antenna structure simulation was 4.78% (735–771 MHz). The simulation of the dipole antenna in the car had a distance of 200 mm, resulting in a frequency range of use of 7.86% (721–780 MHz) as shown in Figure 3. This covered the desired frequency range, but there were also disadvantages in
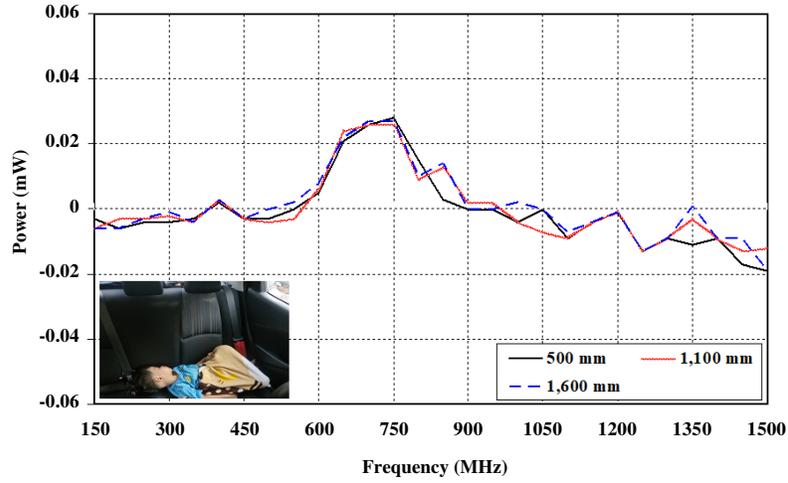
Figure 1. Human body movement detection test.
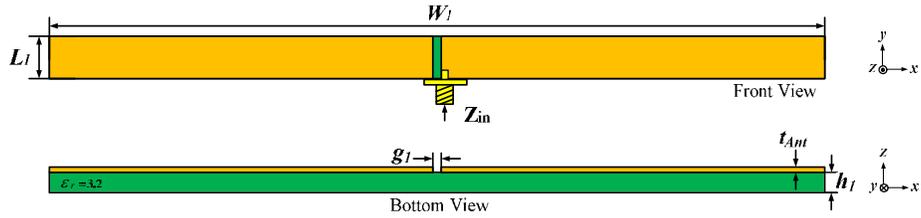
Figure 2. Dipole antenna structure.
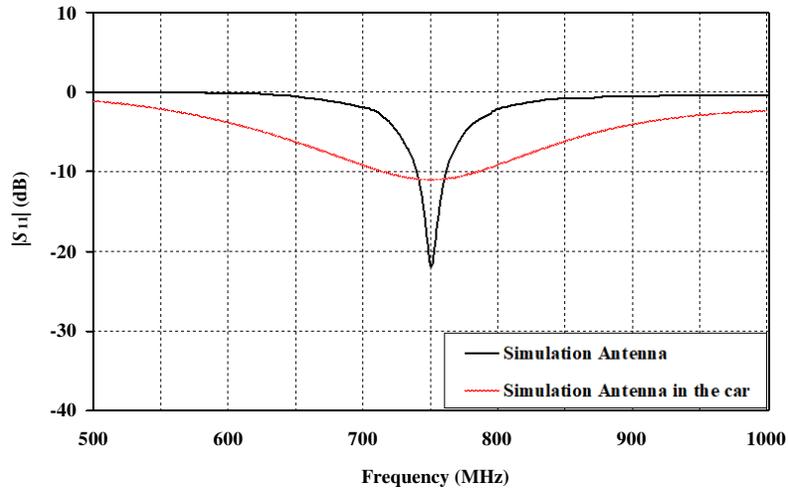
Figure 3. $|S_{11}|$ (dB) value simulation.

the actual installation since too much space was used. The calculation of the antenna width (W_1) was 201.56 mm as shown in Equation (1).

$$W = \frac{0.9c}{f_r \sqrt{\varepsilon_r}} \tag{1}$$

The calculation of the antenna length (L_1) is equal to 12.5 mm as shown in Equation (2).

$$L_1 = \frac{0.031c}{f_r} \tag{2}$$

The calculation of the gap width between the antennas (g_1) is $1.56\,\text{mm}$ as shown in Equation (3).

$$g_1 = \frac{0.39c}{f_r} \tag{3}$$

In simulating the effect of electromagnetic band placement square EBG [35, 36] on the mylar polyester film baseplate, the thickness (t_{EBG}) was $0.297\,\text{mm}$, and the dielectric (ε_r) was 3.2. The electromagnetic band gap structure can be designed with an equivalent circuit consisting of an inductor (L) and a capacitor (C). The resulting capacitor value is the result of the top conductor plate gap. The inductance is derived from the current flowing along the conductors that are close together in circuit LC connected in parallel. The impedance of a parallel resonant circuit can be calculated from Equations (4)–(6) [37].

$$Z = \frac{j\omega L}{1 - \omega^2 LC} \quad : \quad \omega_o = \frac{1}{\sqrt{LC}} \tag{4}$$

The calculation of the capacitor value can be proved by using the technique of calculating the circuit between the capacitor and inductor as shown in Equation (5).

$$C = \frac{W_2 \varepsilon_o \left(1 + \varepsilon_o\right)}{f_r} \cosh^{-1}\left(\frac{2W_2 + g_2}{g_2}\right) \tag{5}$$

The inductance can be calculated from the current flowing through a small wire and conductor as in Equation (6).

$$L = \mu_o t \tag{6}$$

Which found that the result was in the frequency range of use 10.78% (702–$782\,\text{MHz}$), and the width (W_2) and length (L_2) values were $12.5\,\text{mm}$.

(a) Dimensions of metasurface unit cell (b) Equivalent circuit in LC model
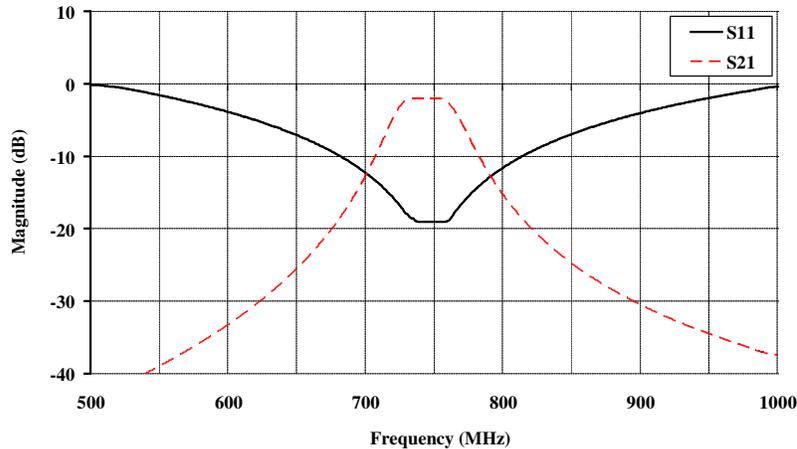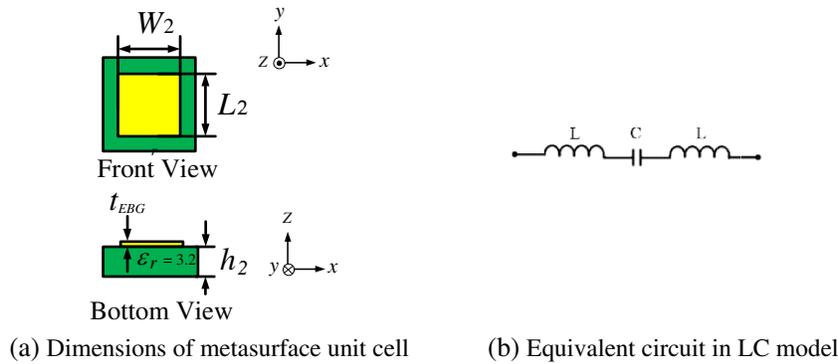
(c) Simulation results of $|S_{11}|$ (dB) and S_{21} (dB) values

Figure 4. Simulation of the effect of a square EBG electromagnetic frequency band placement.

(a) Electromagnetic frequency band (EBG)

(b) Simulating the distance between antennas compatible with EBG plates

(c) Comparison of simulation results of $|S_{11}|$ (dB) values when h_6 was adjusted
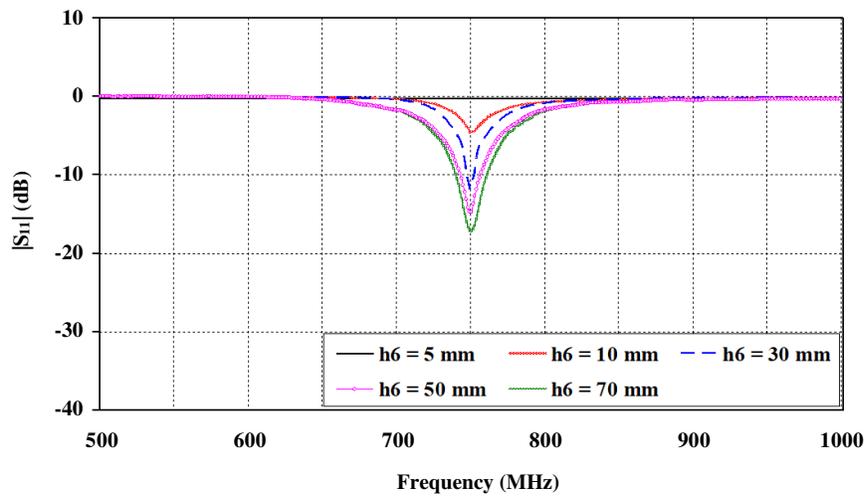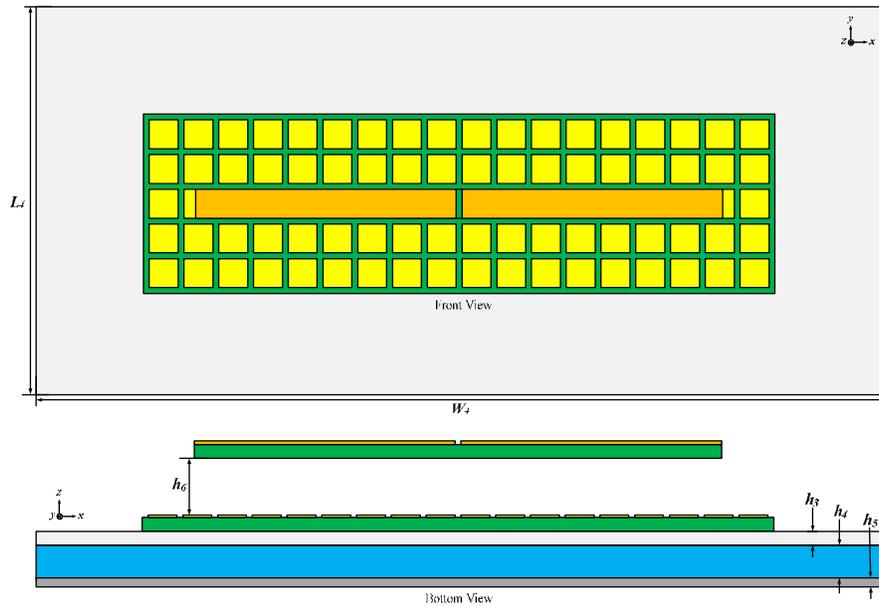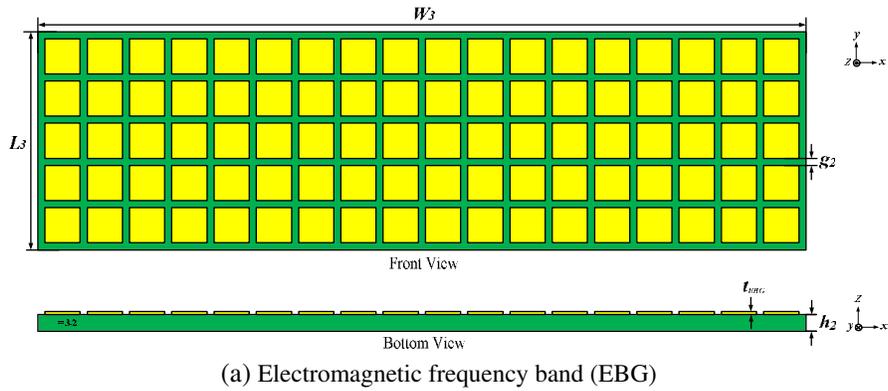
Figure 5. The simulation of the distance between the antenna and the EBG plate is shown with $|S_{11}|$ (dB).

From the design and simulation of the square-shaped EBG plate, it was found that the impedance bandwidth $S_{11} < -10$ dB was 676–814 MHz, and $S_{21} < -10$ dB was equal to 709–778 MHz as shown in Figure 4. From the design and simulation of the square-shaped EBG plate, it was found that the impedance bandwidth $S_{11} < -10$ dB is 676–814 MHz, and $S_{22} < -10$ dB is equal to 709–778 MHz as shown in Figure 4. It has the size of EBG sheet 18×5, placed on the back of the dipole antenna structure. . The width of the gap between the EGB sheets (g_2) was 1.56 mm. When combined, the width (W_3) value was 254.64 mm, and the length (L_3) was 71.86 mm as shown in Figure 5(a). The researchers made the EBG sheet property for MENZ (Mu-Epsilon Near Zero). A positive MENZ value acts as a reflecting surface [36] as shown in Figure 5(b). Distance adjusting was performed based on wavelength values. $0.012\lambda < h_6 < 0.175\lambda$. The range ($h_6$) could be adjusted from 5 mm, 10 mm, 30 mm, 50 mm, and 70 mm. From the adjustment, the closest distance (h_6) was equal to 30 mm, and the dipole antenna had an operating frequency range 1.72% (745–758 MHz) as shown in Figure 5(c) which revealed an increase in gain of 6.70 dBi from 1.67 dBi. Table 1 clearly shows the results. The antenna radiated pattern was compatible with the EBG plate, in the 750 MHz frequency band as shown in Figure 6, and the best parameters are shown in Table 2.

Table 1. Comparison of the measured characteristics of the dipole antenna at 750 MHz.

Dipole antenna		$\|S_{11}\|$ (dB)	VSWR	Gain (dBi)	Z_{in} (Ω)
Simulation	Prototype dipole antenna	-21.61	$1.15:1$	1.67	$51.51 + j12.19$
	Dipole antenna without EBG plate	-10.96	$1.78:1$	3.35	$64.02 - j30.27$
	Dipole antenna compatible with EBG plate, 3 cm spacing	-11.23	$1.66:1$	6.70	$57.62 - j67.64$

Table 2. The value of the variable sizes.

Variable	Meaning	Sizes (mm)
W_1	The width of dipole antenna	201.56
W_2	The width of the base plate of the mylar film EBG sheet	254.64
W_3	The width of the mylar film EBG sheet	12.5
W_4	The width of the steel roof of the car	400
L_1	The length of dipole antenna	12.5
L_2	The length of the base plate of the mylar film EBG sheet	71.86
L_3	The length of the mylar film EBG sheet	12.5
L_4	The length of the steel roof of the car	150
h_1	The thickness of the mylar film base material of the antenna	0.3
h_2	The thickness of the base material of the EBG mylar film sheet	0.3
h_3	The thickness of plastic	2
h_4	The thickness of cloth	5
h_5	The thickness of steel	1.4
h_6	The distance between the dipole antenna and the EBG sheet	30
t_{Ant}	The thickness of the copper dipole antenna	0.297
t_{EBG}	The thickness of the EBG sheet	0.297
g_1	The distance between the dipole antenna and the ground plane	1.56
g_2	The distance between each EBG sheet	1.56

(a) Lateral emission pattern

(b) 3D lateral emission pattern
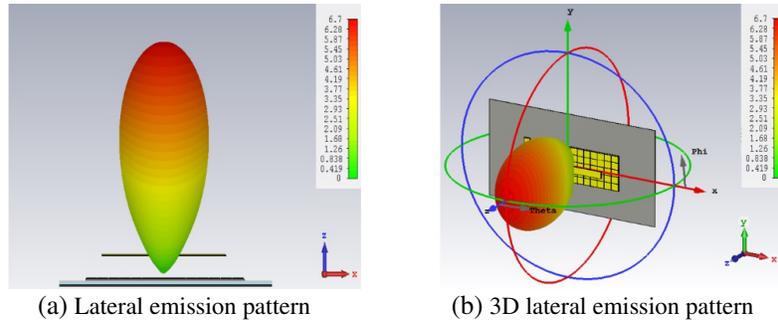
Figure 6. Antenna radiated power scheme in combination with EBG plates.

(a) Dipole antenna

(b) Dipole antenna compatible with EBG plates

(c) Distance between dipole antenna and EBG plate
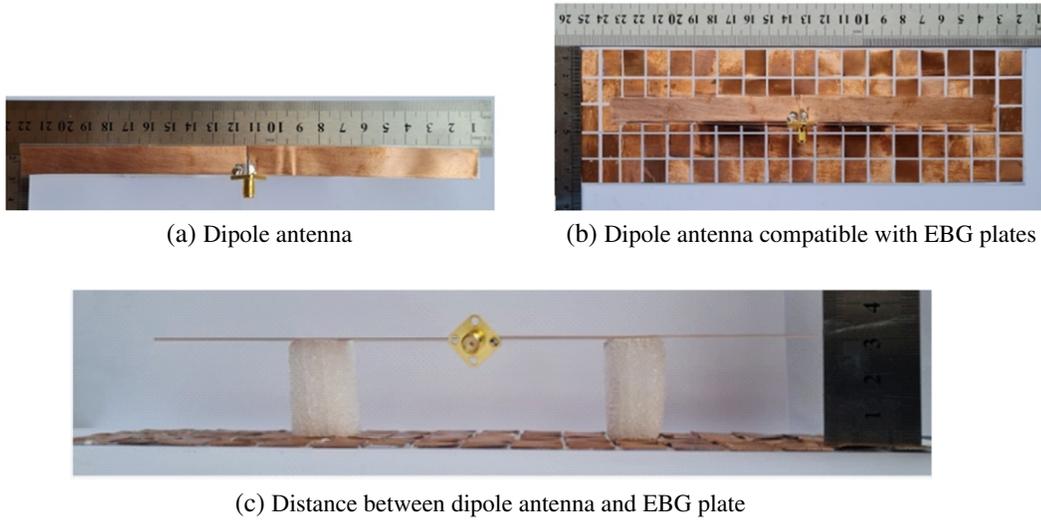
Figure 7. Dipole antenna compatible with an EBG plate.

2.2. Measurement of Antenna Properties

From the design, a dipole antenna was made as shown in Figure 3. The results were measured with Network Analyzer model E5071C and compared with the simulation in terms of reflection coefficient ($S_{11} < -10$ dB), as shown in Figure 7, the standing wave ratio (VSWR), impedance (Z_{in}), and gain. It was found that the actual developed antenna was working in the 750 MHz frequency range as shown in

Table 3. A comparison of the measured properties of a dipole antenna at 750 MHz.

Dipole antenna		$|S_{11}|$ (dB)	VSWR	Gain (dBi)	Z_{in} (Ω)
Simulation	Dipole antenna	-21.61	$1.51:1$	1.67	$51.51 + \text{j}12.19$
	Dipole antenna compatible with EBG plate	-11.23	$1.66:1$	6.70	$57.62 - \text{j}67.64$
Measurement	Dipole antenna	-18.55	$1.38:1$	1.53	$51.51 + \text{j}12.19$
	Dipole antenna compatible with EBG plate	-11.91	$1.59:1$	6.33	$59.61 - \text{j}16.99$
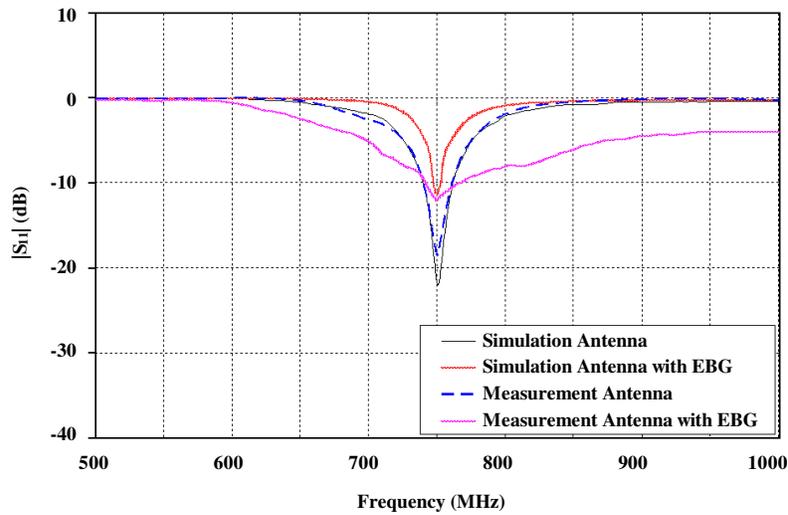
Figure 8. Comparison of simulation results and $|S_{11}|$ (dB) measurement results.

(a) Electric field
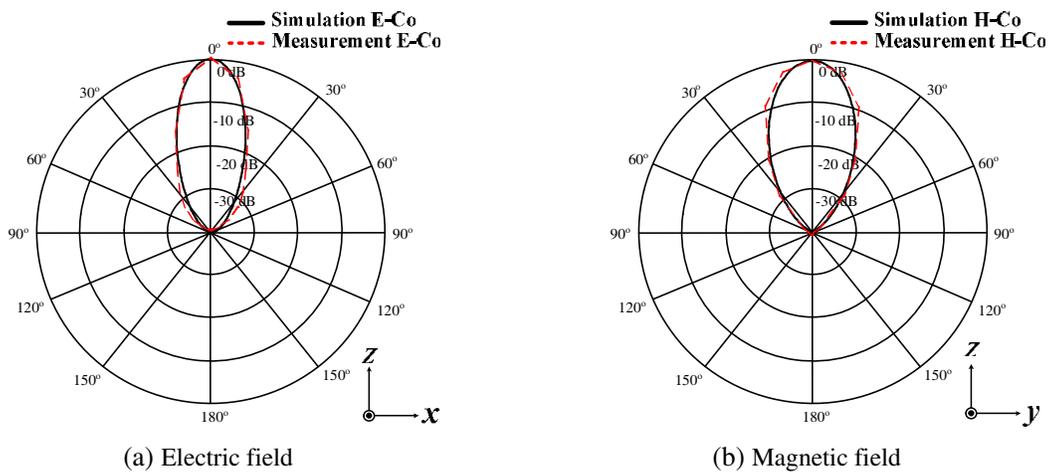
(b) Magnetic field

Figure 9. Comparison of simulation with measurement results of electric and magnetic field radiation patterns.

Figure 8. This had a similar effect to the simulation results of the dipole antenna and was compatible with metamaterials sheet. In addition, it had an advantage in terms of increasing the rate of gain by approximately 3 times, as can be seen in Table 3. The effect of the radiated form at the 750 MHz operating frequency range in the electric field plane and in the magnetic field plane showed a directional pattern of energy radiation pattern which conformed to the plate structure of the metamaterials. That is, in the direction in front of the antenna, it had a similar effect on both planes, as shown in Figure 9.

3. ELECTROMAGNETIC WAVE TEST OF MONITORING CHILDREN TRAPPED IN CARS

Movement was monitored using a V2 NanoVNA transmitter as shown in Figure 10(a), with a signal strength of 0.032 mW. The experiment was done by installing 3 antennas in different positions [7] which were in front of the car at point A, in the center of the car at point B, and behind the car at point C as shown in Figure 10(b). From the test, it was found that the best inspection location was in the center of the car at point B.

At a signal testing distance of 500–1,600 mm, the three cars were 2019 Mazda 2, 2016 Toyota Altis, and 2014 Ford Ranger. From the test, it was found that the signal reception had a change in the signal intensity in body movements at different distances. It was found that at a distance of 500–1000 mm, it had an average signal strength of 0.0318 mW, which differed from a distance of 1,100–1,600 mm with an average signal strength of 0.0293 mW due to the distance and obscuring of the seats on each side.
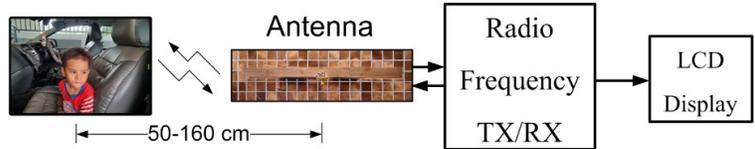
(a) Motion monitoring system
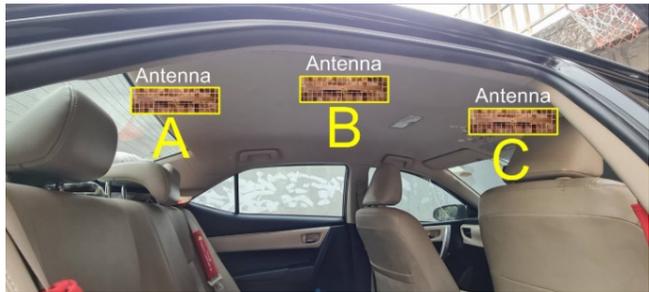
(b) Antenna installation location

Figure 10. Motion monitoring system.

(a) Mazda 2

(b) Toyota Altis

(c) Ford Ranger

Figure 11. Signal test at distance of 500–1,600 mm for all 3 cars.
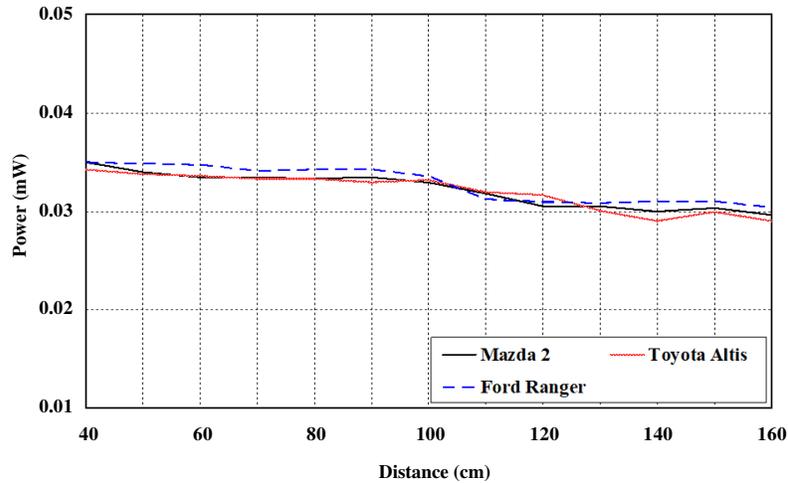
Figure 12. Human body movement detection test 3 models.

In the Ford Ranger, the effect of the signal strength was more than that of both Mazda 2 and Toyota Altis because the structure of the seats is different. This affected the reflection of the signal strength as shown in Figure 11. The 10 experiments per distance shown in Figure 12 were tested at temperatures between 26° and 35° which did not affect the signal strength from the initial test.

4. COMPARISON OF RESEARCH

The study and design of the dipole antenna structure compatible with rectangular EBG plates compared with the previous research are shown in Table 4. It was found that the study had some advantages compared to the other researches: the structural dimensions of the EBG plate, the distance from the dipole antenna to the EBG plate, except [13], 42.30 mm, and a greater gain except research [16]. From the research comparison, the dipole antenna and prototype rectangular EBG plate also had the advantage of being simple and easy to design. The thin structure was lighter due to the use of polyester mylar base plate rather than the mentioned researches.

Table 4. Comparison efficiency of rectenna.

Reference	Frequency (GHz)	Substrate	Antenna size (mm³)	EBG (units)	Thickness (mm)	Gain (dBi)
[9]	1.39–2.09	Rogers	$120 \times 120 \times 0.812$	2×2	16.3	8.2
[10]	2.45/5.20	FR4	$180 \times 180 \times 0.812$	18×18	20.75	9.18/9.75
[11]	2.9–3.32	FR4	$80 \times 80 \times 0.5$	6×6	25	-
[12]	0.868	FR4	$89.4 \times 89.4 \times 1$	8×8	28	5
[13]	0.65–5.00	FR4	$86.4 \times 86.4 \times 0.7$	3×3	42.3	7.52
[14]	4.3–7.6	FR4	$50 \times 50 \times 1.524$	17×17	1.524	5
[15]	1450	Copper	$85 \times 85 \times 3$	17×17	0.003	2.7–4.15
[16]	0.019–0.036	FR4	$1000 \times 1000 \times 1.6$	8×8	18	22.20–16
[21]	4.77–7.12	Metal	$60 \times 60 \times 2$	6×6	4	9.9
[22]	3.04–4.70	Rogers	$80.8 \times 80.8 \times 0.76$	10×10	6.26	10.06/9.98
[24]	3.5–12.4	Denim	$58 \times 80 \times 1$	7×7	3.2	9.1
[26]	2.45	Rogers	$111 \times 111 \times 1.57$	3×3	1	6.8
Proposed	0.75	Polyester mylar	254.64×71.86	18×5	30	6.33

5. CONCLUSION

In this study, a dipole antenna structure combined with an EBG sheet was built to monitor human movement in a car. From the antenna design results, the operating frequency range was 750 MHz, and the best distance between the dipole antenna and the EBG plate was 30 mm, leading to a gain of 6.33 dBi with directional radiation pattern. In the test section, the best place to install an antenna to check the movement of the human body in the car was at a distance of 500–1,600 mm. The antenna had an average signal strength about 0.0335 mW of 10 experiments per distance. This research also found a challenge in the application of the developed antenna to vehicles with more than 7 seats or vans, and this should be used as a basis to develop desired antenna in the future.

ACKNOWLEDGMENT

REFERENCES

1. Glenn, E., T. L. Glenn, and M. L. Neurauter, *Pediatric Vehicular Heatstroke: Review of Literature and Preventative Technologies*, 2019.
2. Ahmad, M. B., A. A. Abdullahi, A. S. Muhammad, Y. B. Saleh, and U. B. Usman, "The various types of sensors used in the security alarm system," *International Journal of New Computer Architectures and their Applications (IJNCAA)*, Vol. 9, No. 2, 50–59, 2019.
3. Razuin, R., M. N. Julina, F. S. Nurquin, and A. H. Amirul, "Heatstroke due to vehicular entrapment: An autopsy case report," *Indian Journal of Forensic Medicine & Toxicology*, Vol. 14, No. 3, 2020.
4. Hammett, D. L., T. M. Kennedy, S. M. Selbst, A. Rollins, and J. E. Fennell, "Pediatric heatstroke fatalities caused by being left in motor vehicles," *Pediatric Emergency Care*, Vol. 37, No. 12, e1560–e1565, 2021.
5. Juan, C. G., E. Bronchalo, B. Potelon, C. Quendo, and J. M. Sabater-Navarro, "Glucose concentration measurement in human blood plasma solutions with microwave sensors," *Sensors*, Vol. 19, No. 17, 3779, 2019.
6. Muñoz-Enano, J., P. Vélez, M. Gil, and F. Martín, "Planar microwave resonant sensors: A review and recent developments," *Applied Sciences*, Vol. 10, No. 7, 2615, 2020.
7. Naktong, W., S. Phonsri, W. Srison, S. Prapakarn, N. Prapakarn, and A. Ruengwaree, "I-shape monopole antenna for applying to check kids trapped inside car," *Engineering, Science, Technology and Architecture Conference, (ESTACON 12)*, 307–312, Thailand, 2021.
8. Kwon, J., H. Park, C. Lee, G. Namgung, Y. Seo, and S. Kahng, "Small EBG decoupling structure for high isolation between two RFID tags," *2019 8th Asia-Pacific Conference on Antennas and Propagation (APCAP)*, 331–336, IEEE, August 2019.
9. Kedze, K. E., H. Wang, S. X. Ta, and I. Park, "Wideband low-profile printed dipole antenna incorporated with folded strips and corner-cut parasitic patches above the ground plane," *IEEE Access*, Vol. 7, 15537–15546, 2019.
10. El Ayachi, M., M. Rahmoun, P. Brachat, and J. M. Ribero, "Realization of planar antenna with wide bandwidth and high gain using novel EBG structure," *2019 International Conference on Wireless Technologies, Embedded and Intelligent Systems (WITS)*, 1–6, IEEE, April 2019.
11. He, R., Z. H. Yan, and Y. B. Meng, "A low-profile dual-polarized crossed dipole antenna on AMC surface," *The Applied Computational Electromagnetics Society Journal (ACES)*, 1038–1042, 2019.

12. Chen, P., L. Wang, and T. Ding, "A broadbiand dual-polarized antenna with CRR-EBG structure for 5G applications," *The Applied Computational Electromagnetics Society Journal (ACES)*, 1507–1512, 2020.

13. Subramanian, S., P. M. Parameswari, and B. Sundarambal, "Design and development of rf energy harvesting loop antenna," *2020 6th International Conference on Advanced Computing and Communication Systems (ICACCS)*, 994–997, IEEE, March 2020.

14. Malhat, H. A. E. A., A. M. Mabrouk, H. El-Hmaily, H. F. Hamed, S. H. Zainud-Deen, and A. A. E. M. Ibrahim, "Electronic beam switching using graphene artificial magnetic conductor surfaces," *Optical and Quantum Electronics*, Vol. 52, No. 7, 1–15, 2020.

15. Tamrakar, M. and U. K. Kommuri, "EBG-AMC-HIS characteristics analysis of QBTR unitcell," *Sādhanā*, Vol. 46, No. 1, 1–6, 2021.

16. Kwon, O. H., W. B. Park, J. Yun, H. J. Lim, and K. C. Hwang, "A low-profile HF meandered dipole antenna with a ferrite-loaded artificial magnetic conductor," *Applied Sciences*, Vol. 11, No. 5, 2237, 2021.

17. Liu, Z. G., R. J. Yin, Z. N. Ying, W. B. Lu, and K. C. Tseng, "Dual-band and shared-aperture Fabry-Perot cavity antenna," *IEEE Antennas and Wireless Propagation Letters*, Vol. 20, No. 9, 1686–1690, 2021.

18. Malekpoor, H. and M. Hamidkhani, "Performance enhancement of low-profile wideband multi-element MIMO arrays backed by AMC surface for vehicular wireless communications," *IEEE Access*, Vol. 9, 166206–166222, 2021.

19. Malekpoor, H. and A. Abolmasoumi, "Gain and isolation improvement of compact MIMO printed dipole arrays realized by second iteration Giuseppe Peano AMC for 4G/5G wireless networks," *Wireless Networks*, 1–14, 2022.

20. Jiang, C., S. Wang, T. Wei, Q. Yang, J. Li, and E. Chen, "Dual-band circularly polarized crossed-dipole antenna backed by a double layer artificial magnetic conductor," *2020 IEEE 3rd International Conference on Electronic Information and Communication Technology (ICEICT)*, 217–220, IEEE, November 2020.

21. Jiang, Z., Z. Wang, L. Y. Nie, X. Zhao, and S. Huang, "A low-profile ultra-wideband slotted dipole antenna based on artificial magnetic conductor," *IEEE Antennas and Wireless Propagation Letters*, Vol. 21, No. 4, 6710–675, 2022.

22. Xiong, H. Q., C. J. Zhang, and M. S. Tong, "Wideband low-profile dual-polarized antenna based on a gain enhanced EBG reflector," *IEEE Transactions on Components, Packaging and Manufacturing Technology*, 391–394, 2021.

23. Ashyap, A. Y., Z. Z. Abidin, S. H. Dahlan, H. A. Majid, M. R. Kamarudin, A. Alomainy, and J. M. Noras, "Highly efficient wearable CPW antenna enabled by EBG-FSS structure for medical body area network applications," *IEEE Access*, Vol. 6, 77529–77541, 2018.

24. Yalduz, H., B. Koç, L. Kuzu, and M. Turkmen, "An ultra-wide band low-SAR flexible metasurface-enabled antenna for WBAN applications," *Applied Physics A*, Vol. 125, No. 9, 1–11, 2019.

25. Amalraj, T. D. and R. Savarimuthu, "Design and analysis of microstrip patch antenna using periodic EBG structure for C-band applications," *Wireless Personal Communications*, Vol. 109, No. 3, 2077–2094, 2019.

26. Jun, S., B. Sanz-Izquierdo, and E. A. Parker, "A novel reconfigurable EBG structure and its potential use as liquid sensor," *2019 13th European Conference on Antennas and Propagation (EuCAP)*, 1–5, IEEE, March 2019.

27. Bora, P., P. Pardhasaradhi, and B. T. P. Madhav, "Design and analysis of EBG antenna for Wi-Fi, LTE, and WLAN applications," *The Applied Computational Electromagnetics Society Journal (ACES)*, 1030–1036, 2020.

28. Zhang, K., G. A. Vandenbosch, and S. Yan, "A novel design approach for compact wearable antennas based on metasurfaces," *IEEE Transactions on Biomedical Circuits and Systems*, Vol. 14, No. 4, 918–927, 2020.

29. Doğan, G. T. and E. Tetik, "Metamaterial based flexible coplanar antenna design and simulation for human body applications," *Journal of the Institute of Science and Technology*, Vol. 10, No. 4, 2541–2550, 2020.

30. El May, W., I. Sfar, J. M. Ribero, and L. Osman, "Design of low-profile and safe low SAR tri-band textile EBG-based antenna for IoT applications," *Progress In Electromagnetics Research Letters*, Vol. 98, 85–94, 2021.

31. Patil, S., Verma, A., A. K. Singh, B. K. Kanaujia, and S. Kumar, "A low-profile circularly polarized microstrip antenna using elliptical electromagnetic band gap structure," *International Journal of Microwave and Wireless Technologies*, 1–10, 2021.

32. Ramanpreet, N., M. Rattan, and S. S. Gill, "Compact and low profile planar antenna with novel metastructure for wearable MBAN devices," *Wireless Personal Communications*, Vol. 118, No. 4, 3335–3347, 2021.

33. Arif, A., M. R. Akram, K. Riaz, M. Zubair, and M. Q. Mehmood, "Koch fractal based wearable antenna backed with EBG plane," *2020 17th International Bhurban Conference on Applied Sciences and Technology (IBCAST)*, 642–646, IEEE, January 2020.

34. Balanis, C. A., *Antenna Theory and Design*, John Willey & Sons, NY, USA, 1997.

35. Fhafhiem, N., P. Krachodnok, and R. Wongsan, "Curved strip dipole antenna on EBG reflector plane for RFID applications," *WSEAS Transactions on Communications*, Vol. 9, No. 6, 374–383, 2010.

36. Naktong, W., A. Ruengwaree, N. Fhafhiem, and P. Krachodnok, "Resonator rectenna design based on metamaterials for low-RF energy harvesting," *CMC-Computers Materials & Continua*, Vol. 68, No. 2, 1731–1750, 2021.

37. Malekpoor, H. and M. Hamidkhani, "Performance enhancement of low-profile wideband multi-element MIMO arrays backed by AMC surface for vehicular wireless communications," *IEEE Access*, Vol. 9, 166206–166222, 2021.